JCTC Journal of Chemical Theory and Computation

Atomic Level Anisotropy in the Electrostatic Modeling of Lone Pairs for a Polarizable Force Field Based on the Classical Drude Oscillator

Edward Harder,[†] Victor M. Anisimov,[‡] Igor V. Vorobyov,[‡] Pedro E. M. Lopes,[‡] Sergei Y. Noskov,[†] Alexander D. MacKerell Jr.,*[,‡] and Benoît Roux*[,†]

Institute for Molecular Pediatric Sciences, Gordon Center for Integrative Science, University of Chicago, Chicago, Illinois 60637, and Department of Pharmaceutical Sciences, School of Pharmacy, University of Maryland, Baltimore, Maryland 21201

Received May 23, 2006

Abstract: Electron pairs in the valence shell of an atom that do not participate in the bonding of a molecule ("lone pairs") give rise to a concentrated electron density away from the atom center. To account for the asymmetry in the electron charge density that arises from lone pairs, an electrostatic model is developed that is parametrically anisotropic at the atomic level. The model uses virtual interaction sites with partial charges that are associated but not coincident with the nuclei. In addition, the model incorporates anisotropic atomic polarizabilities. The protocol previously outlined in Anisimov et al. [*J. Chem. Theory Comput.* **2005**, *1*, 153] for parametrizing the electrostatic potential energy of a polarizable force field using classical Drude oscillators is extended to incorporate additional lone pair parameters. To probe the electrostatic environment around the lone pairs, the static (molecule alone) and perturbed (molecule in the presence of a test charge) electrostatic potential (ESP) are evaluated and compared to high level quantum mechanical (QM) electronic structure calculations. The parametrization of the virtual sites relies on data from the QM static ESP. The contribution to the perturbed ESP from the electronic polarization of the molecule is used to resolve the components of the atomic polarizability tensor. The model is tested in the case of four molecules: methanol, acetone, methylamine, and pyridine. Interaction energies with water and sodium are used to assess the accuracy of the model. The results are compared with simpler models placing all the charge on the nuclei as well as using only isotropic atomic polarizabilities. Analysis shows that the addition of virtual sites reduces the average error relative to the QM calculations. In contrast to models with atom centered charges, the virtual site models correctly predict the minimum energy conformation for acetone and methanol, with water, to be closely coordinated with the lone pair direction. Furthermore, addition of anisotropic atomic polarizabilities to the virtual site model allows for precise fitting to the local perturbed QM ESP.

1. Introduction

Computer simulations of atomistic models used to investigate biological phenomena often employ simple potential functions that balance computational efficiency with a suitable level of accuracy for the microscopic interactions. Commonly used models such as CHARMM,[1] OPLS/AA,[2] AMBER,[3] and GROMOS[4] approximate the electrostatic potential that surrounds a molecule by using point charges of fixed magnitude placed on (or coordinated to) atomic positions. The underlying assumption in such models is that the electron density of the molecule remains unaffected by external perturbations. However, it is well-understood that the electron density of real molecules is not static but responds to fluctuating electric

* Corresponding author e-mail: roux@uchicago.edu alex@outerbanks.umaryland.edu.
[†] University of Chicago.
[‡] University of Maryland.

10.1021/ct600180x CCC: $33.50 © 2006 American Chemical Society
Published on Web 10/21/2006

fields arising from neighboring entities. Even in neat liquid water such fluctuations are significant and comparable in magnitude to the size of the induced molecular dipole (≈1 D).[5] The importance of these effects in the case of biological macromolecular systems, with variations in microscopic environments ranging from hydrophobic to highly polar, is expected to be considerable. The need for explicit inclusion of induced polarization effects has been explicitly documented in studies concerned with the structural rearrangements in liquid water,[6−8] the hydration of small ions,[9−13] the structure of water−alcohol liquid mixtures,[14] the dielectric constant of pure nonpolar solvents,[15] the solvation of water around a protein surface with varying polarity,[16] and the conduction of ions through a membrane channel.[17,18]

To make progress toward the parametrization of a polarizable biomolecular force field we have chosen to represent electronic induction using classical Drude oscillators.[15,19−21,48] Similar to commonly used inducible point dipole models,[22−27] Drude oscillators represent electronic induction using a pair of charges of equal magnitude and opposite sign connected by a harmonic spring.[28] In the present model the Drude spring connects the negative Drude charge to its associated heavy atom. The familiar self-consistent field (SCF) condition of induced polarization is reproduced if the massless particles are allowed to relax instantaneously to their local energy minima for any given fixed configuration of the atoms in the system. The model reduces to the standard model with induced point dipoles in the limit of a large spring constant. For simplicity, the initial implementation of the polarizable force field with classical Drude oscillators assumed that the fixed charges were centered on the nuclei and that the local atomic polarizabilities were isotropic.[21] Models parameterized in accordance with this framework show good agreement with experimental properties, including the diffusivity and dielectric constant of ethanol/water mixtures[14] and crystal structures of DNA.[21] Nevertheless, it may be necessary to go beyond this basic framework to achieve the needed level of accuracy for detailed microscopic interactions. In particular, the presence of nonbonding electronic density situated away from the nucleus, so-called "lone pairs", breaks the spherical symmetry assumed by the atom-centered electrostatic models. It is intuitively obvious that that the local electrostatic field arising from lone pairs could be poorly described by an atom-centered centrosymmetric model. Furthermore, it is likely that induced electronic polarization in the neighborhood of the lone pairs is anisotropic. In a rational effort to develop a computationally useful and accurate force field, a quantitative characterization is essential.

The goal of this article is to address these issues. The strategy employed in the current effort focuses primarily on the accuracy of microscopic interactions rather than the properties of the bulk phase. The target interaction data, used to fit the electrostatic model, are supplied by high level electronic structure calculations of the surrounding electrostatic potential (ESP). The performance of three electrostatic models at different levels of complexity is examined: an atom-centered charge model with isotropic Drude oscillators, a model with virtual sites representing the lone pairs and isotropic Drude oscillators, and a model with virtual sites representing the lone pairs together with anisotropic Drude oscillators. The ability of the different electrostatic models to accurately represent microscopic interactions is examined in the case of four molecules: methanol, acetone, methylamine, and pyridine. The details of the model are presented in section 2.1. The parameter fitting protocol, generalized to include anisotropic atomic polarizabilities and virtual sites, is given in section 2.2, and all remaining computational details are described in section 3. Section 4.1 presents a general discussion of the electrostatic properties associated with lone pairs. An examination of the validity of a linear polarization response is presented in section 4.3. Dimer energies with water and sodium and a comparison between QM and the MM models is presented in section 4.2. The paper is concluded with a summary of the main results and an outlook for future force field development.

2. Methods

2.1. Model. To model the electronic polarization of a given atom, a mobile auxiliary particle carrying a charge q^D is introduced and attached to the atom by a harmonic spring. A charge of opposite sign is added to the atom and the electroneutral pair forms a classical Drude oscillator, which polarizes in response to an external field. In the present implementation, the charge of the mobile Drude particle is chosen to be negative,[15,21,48] because this yields a more realistic electrostatic response in molecular systems (see also the discussion in section 4.3 below). The model comprises the "core" charges q_i, associated either with atomic or virtual lone pair sites, as well as the Drude charges q_i^D and $-q_i^D$, associated with the electroneutral oscillators. For a fixed atomic geometry, the electrostatic response of a molecule is determined by the potential energy

$$U_{\text{Drude}} = U_{\text{self}} + U_{\text{elec}} \tag{1}$$

The first term in eq 1 is the harmonic self-energy of the Drude oscillators. For a given oscillator, it can be written as

$$\begin{aligned} U_{\text{self}} &= \frac{1}{2}\mathbf{d}\cdot\mathbf{K}^{(D)}\cdot\mathbf{d} \\ &= \frac{1}{2}([\mathbf{K}_{11}^{(D)}]d_1^{\,2} + [\mathbf{K}_{22}^{(D)}]d_2^{\,2} + [\mathbf{K}_{33}^{(D)}]d_3^{\,2}) \end{aligned} \tag{2}$$

where d_1, d_2, and d_3 are the projection of the Drude displacement vector $\mathbf{d}$ on orthogonal axis defined using a local intramolecular reference frame. For example $d_1 = \mathbf{d}\cdot\hat{n}_{A,B}$ where $\hat{n}_{A,B}$ is a unit vector directed between atoms A and B in the molecule of interest. One may note that, due to the intramolecular electrostatic interactions between induced oscillators, even a model with isotropic spring constants can give rise to a molecular polarizability that is anisotropic. However, further analysis shows that this level of anisotropy is inadequate to properly model the local anisotropy around lone pairs. This generalization to anisotropic atomic polarizabilities has been implemented in CHARMM.[31]

The second term, U_{elec}, corresponds to the sum over all Coulombic interactions between the core charges q_i located at $\mathbf{r}_i$ and the Drude charges q_i^D and $-q_i^D$, located at $\mathbf{r}_i$, and

$\mathbf{r}_i^D = \mathbf{r}_i + \mathbf{d}_i$, respectively. The interactions of the various pairs of charges are treated according to the topological bonding order determined from the atoms in the molecule. As in standard force fields, the interactions between core charges corresponding to 1−2 and 1−3 pairs are excluded. Similarly, the interactions of the Drude oscillators with core charges are excluded for 1−2 and 1−3 pairs. The interactions involving all core charges and all Drude oscillators are included without screening for all 1−4 pairs and beyond. The interactions of the Drude oscillators corresponding to 1−2 and 1−3 pairs are screened by the function S_{ij}

$$S_{ij}(r_{ij}) = 1 - \left(1 + \frac{ar_{ij}}{2(\alpha_i\alpha_j)^{1/6}}\right)e^{-ar_{ij}/(\alpha_i\alpha_j)^{1/6}} \quad (3)$$

It should be noted that the screening is applied to the interaction of the electroneutral pair, including both the mobile charge q^D and its countercharge $-q^D$ located on the atom. The empirical dimensionless coefficient a is chosen to be 2.6, consistent with previous work.[19,29,30]

In accord with the Born−Oppenheimer approximation in quantum mechanics, the electronic degrees of freedom in the model are relaxed to their energy minimum for any given nuclear configuration. The result is an equilibrium between the force of the Drude spring and the electrostatic force from the total external electric field, $\mathbf{K}_i^D\mathbf{d}_i = -q_i^D\mathbf{E}_i$, where $\mathbf{E}_i$ is the total electric field at the position of the Drude particle, $\mathbf{r}^D$. This condition can be written in a form analogous to the self-consistent field (SCF) equation for atomic point dipoles, $\mu_i = \alpha_i\mathbf{E}_i$. This yields the definition of the atomic polarizability tensor as $\alpha_i = (q_i^D)^2[\mathbf{K}^D]^{-1}$.

Three models are constructed with these fundamental elements: an atom-centered charge model with isotropic Drude oscillators denoted NOLP+ISO, a model with virtual lone pair sites and isotropic Drude oscillators denoted LP+ISO, and a model with virtual lone pair sites and anisotropic Drude oscillators denoted LP+ANISO.

2.2. Parameter Fitting Protocol. The parametrization protocol for the core charges and polarizabilities used in the present work is an extension of the method documented by Anisimov et al.[21] The parametrization is achieved by comparison to analogous QM electronic structure computations. The ESP map is computed on a set of grid points surrounding the molecule. To measure the electronic response, a series of perturbed ESP maps is computed by placing a single $+0.5e$ test charge at chemically relevant positions around the molecule. The same calculation is repeated using our MM model, restricting the atomic polarizabilities to be isotropic. The approach is similar in spirit to work by Friesner and co-workers used in the parametrization of polarizable point dipole and fluctuating charge models.[27,32−35] The set of electrostatic parameters (charges and polarizabilities) is obtained by optimizing the function

$$\chi^2[\alpha, q] = \sum_{p,grid}[\phi_{p,grid}^{QM} - \phi_{p,grid}^{MM}]^2 + \chi_r^2 \quad (4)$$

where the index p sums over different positions of the test charge around the model compound. Eq 4 measures the deviations of the ESP between the MM and QM results. The optimal parameters are determined with an additional restraint, χ_r^2. Such a restraint is necessary because the charge fitting problem is underdetermined,[36,37] and an unrestrained fit (though it may fit the ESP well at the grid points) can often lead to a set of charges with poor chemical significance and limited usefulness for a force field. This problem is particularly evident with buried atoms whose partial charges contribute little to the ESP.[36] The restrained fitting scheme employed here is similar to the RESP scheme of Bayly et al.[37] The χ_r^2 term in eq 4 provides a penalty for deviations of the fitted parameters relative to chosen reference values. The functional form of the restraint potential is a flat well potential and deviations within a defined interval $|q_{ref} - q_{flat}, q_{ref} + q_{flat}|$ receive no penalty, while larger deviations feel a parabolic restraint given by

$$\chi_r^2 = \sum_i w_i[q_i - q_{ref,i}]^2 \quad (5)$$

where w is a weighting factor for the restraint. The reference values are adopted from two sources. The PARAM22 force field of CHARMM[1,38,39] is used to provide a set of reference values for the atomic charges.[21] The atomic polarizabilities of Miller,[40] derived from experimental gas-phase molecular polarizabilities, are used as a reference for the Drude oscillator parameters. The Miller parameters assign additive atomic polarizabilities to atom types based on the hybridization state of the atom including hydrogen atoms. The reference polarizabilities were constructed by adding the Miller polarizabilities of hydrogen atoms to their covalently bonded heavy atom.[21]

The MM models containing virtual sites and anisotropic polarizabilities have additional parameters (geometry of the virtual sites and the components of the force constant tensor) that must be fitted to QM data. The virtual site geometry is determined iteratively using the aforementioned charge/polarizability fitting procedure. An initial guess is obtained from an atoms in molecules (AIM)[41] analysis of the electron density, by which the positions of lone pairs can be mapped to local maxima in the negative of the Laplacian of the density. The charges are then fit using the above protocol. The reference charge values for the lone pair containing atoms are shifted to the virtual sites, and the charge on the corresponding atom site is restrained to zero during the fitting procedure. Further refinement of the lone pair positions is accomplished by comparing the static (unperturbed) ESP, ϕ_{stat}, along an arc spanning a plane containing the lone pair(s) at a distance of 2 Å from the reference atom (i.e. oxygen or nitrogen for the molecules studied) site. Using this geometry, all core charges and isotropic atomic polarizabilities are resolved from the RESP electrostatic potential fitting procedure outlined above. The generalization to anisotropic atomic polarizabilities in the model requires an additional step in the parametrization process. A $+0.5e$ test charge is placed on the arc positions, and the perturbed ESP (ϕ_{pert}) is evaluated at the position of the test charge. Defining the contribution arising from the polarization of the molecule in response to external perturbation as ϕ_{pol}, equal to the difference between the perturbed and unperturbed ESP, the

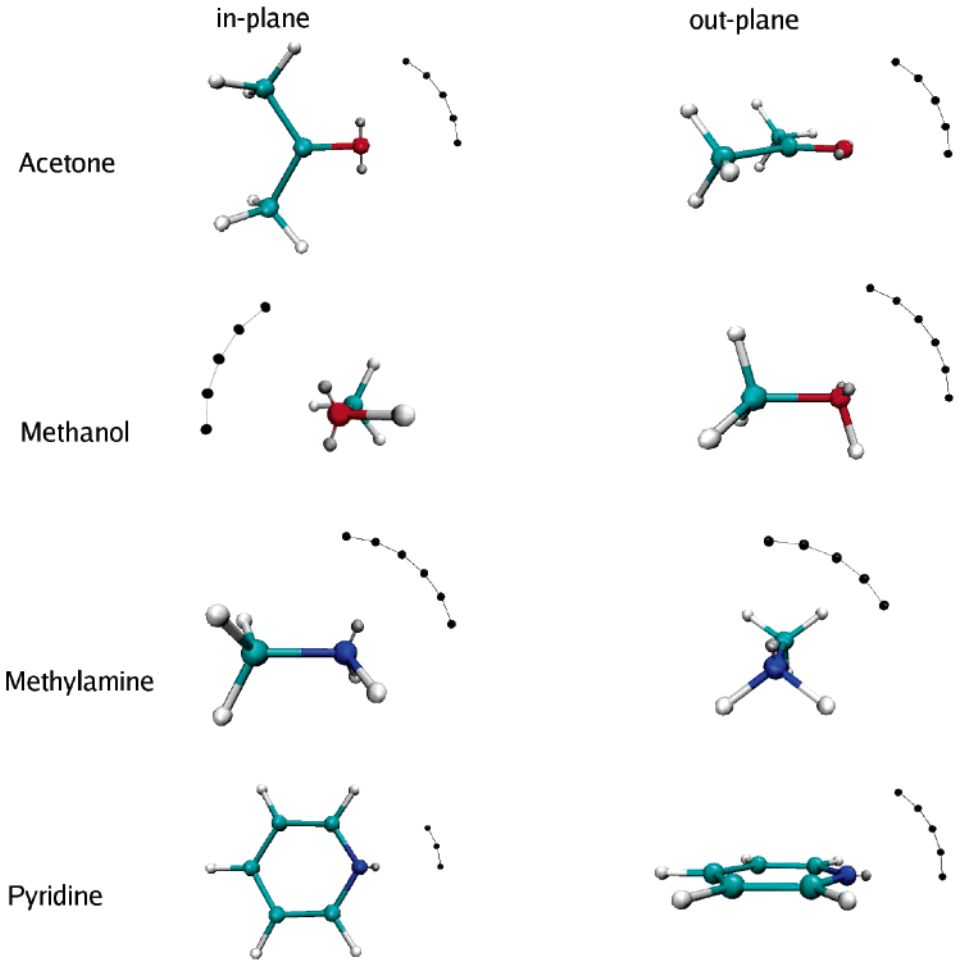

Figure 1. Location of arc point positions used to probe the local ESP. The arc point positions are represented by black spheres.

components of the force constant matrix **K** are determined, through a trial and error procedure, to match the QM result for ϕ_{pol}.

The atom LJ parameters, with the exception of oxygen or nitrogen, are taken from the PARAM22 force field of CHARMM.[1,38,39] For interaction energies with water, the LJ parameters on oxygen or nitrogen are varied to best reproduce the QM interaction energies. For interaction energies with the sodium cation, the LJ on the oxygen or nitrogen and if necessary the LJ parameters on the virtual sites are varied to best reproduce the QM interaction energies. The model parameters are given in the Supporting Information.

3. Computational Details

QM calculations were carried out using the Gaussian 03 suite of programs.[42] The first step in the parametrization is to obtain optimized geometries. The MP2(fc)/6-31G(d) level of theory and basis set found to give molecular geometries consistent with experiment[43] was used in the present work.

The QM ESP maps were evaluated using density functional theory with the B3LYP functional[44,45] and the aug-cc-pVDZ basis set. This combination has been shown to give good agreement with molecular polarizabilities and gas-phase dipole moments.[21] Minimization of eq 4 to arrive at the electrostatic parameters of the force field was carried out using the FITCHARGE module in CHARMM.[31] The QM ESP arcs used to parametrize the virtual site location, and polarizability components of the anisotropic Drude oscillator were also evaluated using the B3LYP/aug-cc-pVDZ combination.

Optimized interaction energies and geometries for the model compounds with individual water molecules or sodium ions were obtained by minimizing along selected intermolecular distance coordinates while keeping the geometries of the model compounds and water fixed. The interaction energy is evaluated as the difference between the resultant minimum energy conformer and the respective monomers. MP2 calculations with the 6-311+G* basis set were done to locate the position of the minima for each dimer (both water and sodium). This was followed by MP2 calculations with the 6-311+G(3df,2p) basis set and the removal of basis set superposition error.[46] Polarization and diffuse functions were included to give a faithful representation of the polarization response. The LJ minimum for the MM models was varied until good agreement for the lowest energy conformation was achieved.

Computations designed to probe the breakdown of linear response used electrostatic perturbations with a test charge as large as 2.0*e* within 2 Å of the carbonyl oxygen of acetone. To achieve an accurate representation of the electronic response in the presence of such a large perturbation, MP2 calculations with the 6-311+G(3df,2p) basis set were again used in the evaluation of ϕ_{stat}, ϕ_{pol}, and the interaction energy.

The size of the force constant in eq 2 is not a variable in

the parameter optimization. The value is chosen to be sufficiently large such that Drude oscillator displacements, for typical field strengths found in biomolecular systems, remain small relative to interatomic distances. This is done to ensure that the model does not deviate strongly from the point dipole limit. Previous work with an isotropic polarizable Drude model of water used a value of $k_D = 1000$ kcal/mol/Å^2.[19] Consistent with this choice the components of the anisotropic Drude oscillators were chosen so that the trace of the tensor has a similar value (i.e. tr$\{\mathbf{K}_D\} \approx 1000$ kcal/mol/Å^2).

4. Results and Discussion

4.1. Parametrization and the Electrostatic Potential Arcs. The ESP calculated along "in-plane" and "out-plane" arcs, used to probe the electrostatic environment of the lone pairs, are defined by two angles and the distance from the reference heavy atom. For acetone and methanol, the in-plane arc spans a plane containing both virtual sites and the reference heavy atom. For methylamine and pyridine the in-plane arc spans a plane containing the virtual site and the heavy atoms of the molecule. The in-plane arc, which varies with the angle θ, is illustrated in Figure 1 for each molecule. The out-plane arc spans a plane orthogonal to the first. The out-plane arc, which varies with the angle Φ, is shown in Figure 1 for each molecule. In the figure, the arc point positions are represented by black spheres. For acetone, methylamine, and pyridine θ is the C−O−X (or C−N−X) angle, where C is the carbonyl carbon of acetone or the carbon 4 atom of pyridine and X denotes positions along the arc. The angle Φ is defined by the $X_{in-plane}$−O−X (or $X_{in-plane}$−N−X) positions where $X_{in-plane}$ is the in-plane arc position at $\theta = 180$ for acetone and pyridine and $\theta = 105$ for methylamine. For methanol Φ is the C−O−X angle and θ is the $X_{out-plane}$−O−X (or $X_{out-plane}$−N−X) angle where $X_{out-plane}$ is at $\Phi = 105$. The total ESP at the position of the 0.5e test charge is presented in panel C of Figures 2−5 for the four molecules. The static and polarization contributions to the ESP are presented in panels A and B, respectively. In each plot the black solid line is the QM result, the red dashed line is the model optimized using the original protocol (NOLP+ISO), the green solid line is the MM model with virtual sites and isotropic Drude oscillators (LP+ISO), and the blue-cross line is the MM model with virtual sites and anisotropic Drude oscillators on the reference heavy atoms (LP+ANISO).

The position of the virtual sites is not part of the function minimized in the charge fitting protocol (see eq 4). As stated in section 2.2, an initial guess for the virtual site geometry follows from an AIM analysis of the electron density. In an iterative process the geometry is modified followed by the minimization of eq 4 until qualitative agreement between the QM ϕ_{stat} and the MM ϕ_{stat} (see panel A) is obtained. This is the LP+ISO model. The final virtual site geometries of each model are reported in the Supporting Information. The improved agreement between QM and the MM models using virtual sites with respect to the in-plane arcs is clear for all four molecules. The NOLP MM models do not give a strong enough ϕ_{stat} at arc positions that are approximately coordinated with the lone pairs ($\theta = 120$ for acetone, $\theta =$ 60 for methanol, $\theta = 110$ for methylamine, and $\theta = 180$ for pyridine). This is corrected by the addition of virtual sites, which yields an unperturbed ESP in better agreement with the QM result. It may be noted that the LP+ANISO and LP+ISO models are nearly equivalent with respect to the unperturbed ESP, making only the plot for LP+ANISO visible in the plots. Similar improvement is also seen for the out-plane arc in methylamine and pyridine where addition of a virtual site increases the strength of ϕ_{stat} along the lone pair direction leading to improved agreement with the QM static ESP. For acetone and methanol it appears that the orthogonal out-plane arc is already well represented by the NOLP models, and addition of the virtual site provides little improvement.

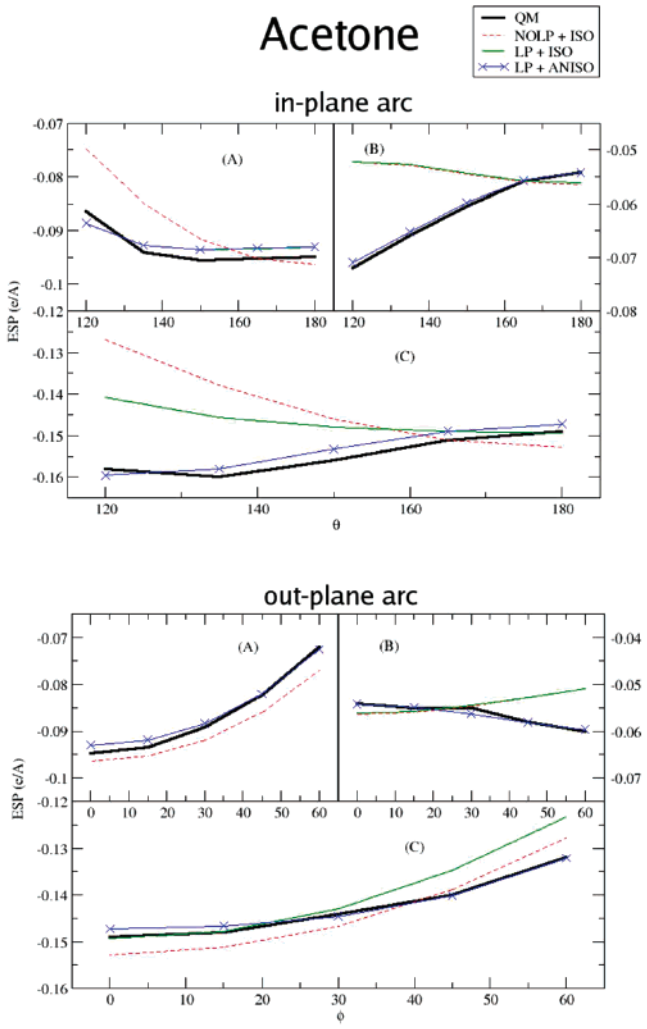

Figure 2. The ESP along an arc 2 Å from the oxygen of an acetone monomer is plotted in panel (A). The polarization contribution and total ESP from acetone in the presence of a 0.5e test charge is plotted in panels (B) and (C), respectively. The perturbed ESP is calculated at the position of the 0.5e test charge.

The plots of the polarization ESP (panel B) show the effect lone pairs have on the electronic response of the molecule. The standard MM model, which uses isotropic atomic polarizabilities (ISO), gives a response along the arc that is approximately uniform. Some anisotropy is present in the response of the ISO models due to the screened Coulomb

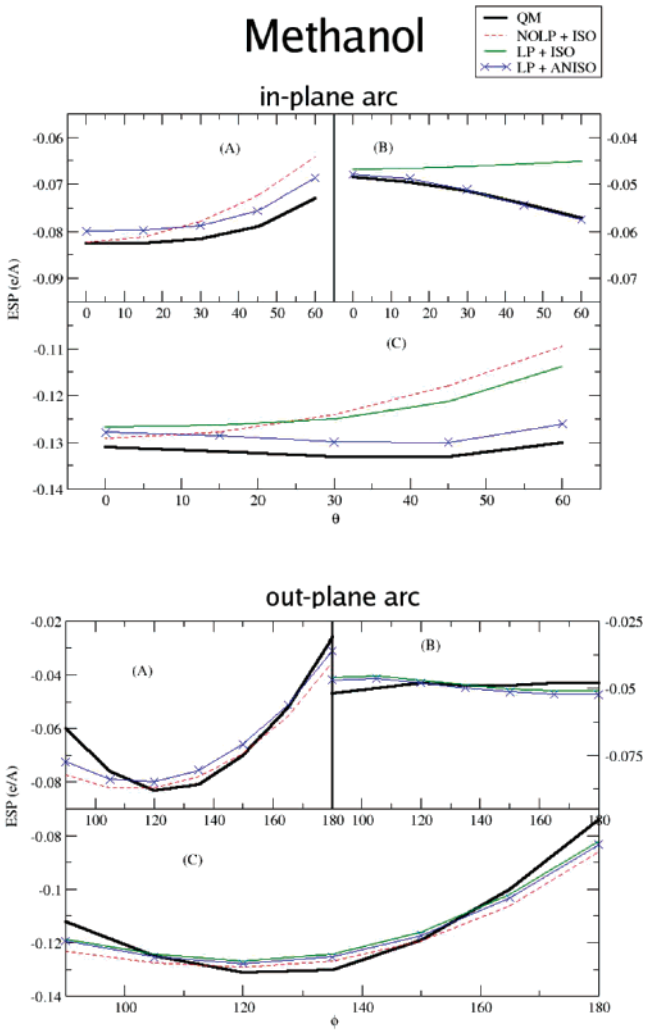

Figure 3. The ESP along an arc 2 Å from the oxygen of an methanol monomer is plotted in panel (A). The polarization contribution and total ESP from methanol in the presence of a 0.5*e* test charge is plotted in panels (B) and (C), respectively. The perturbed ESP is calculated at the position of the 0.5*e* test charge.

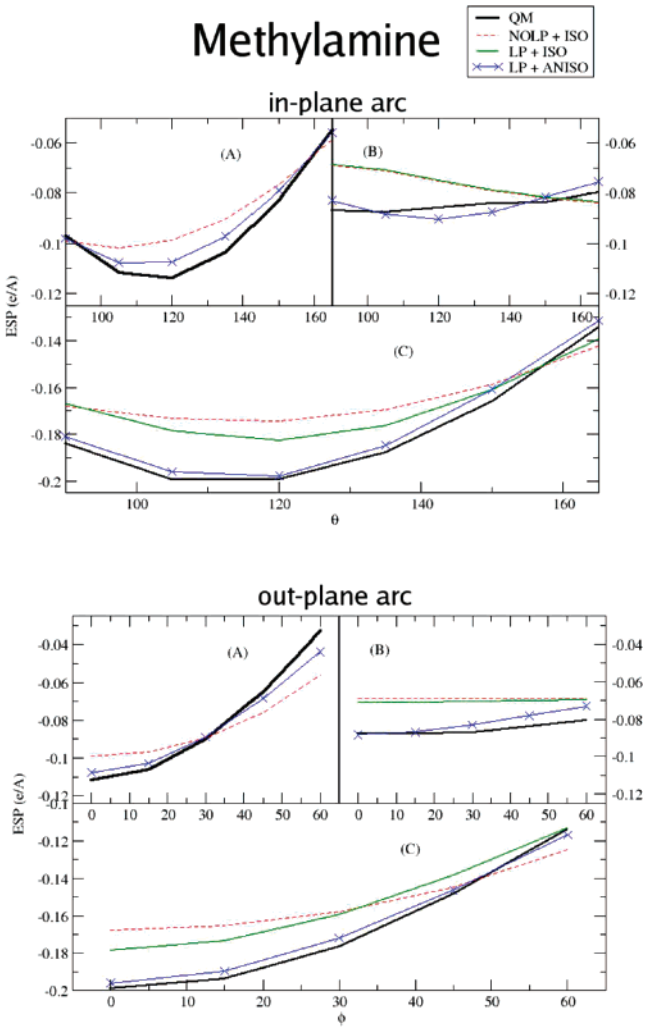

Figure 4. The ESP along an arc 2 Å from the nitrogen of an methylamine monomer is plotted in panel (A). The polarization contribution and total ESP from methylamine in the presence of a 0.5*e* test charge is plotted in panels (B) and (C), respectively. The perturbed ESP is calculated at the position of the 0.5*e* test charge.

interactions between induced Drude dipoles. However, over the local coordinates probed by the arcs, this effect is small and qualitatively opposes the trend seen in the anisotropy of the QM response. The local QM response reflects a stronger polarization around the lone pair regions, which seems intuitive given the greater electron density in that region. The magnitude in the discrepancy between the standard MM model and QM is not small for the 0.5*e* test charge. In fact for the in-plane arc of acetone the difference in the ESP is approximately 0.02 e/Å comparable in magnitude to the improvement found in the static field by the addition of virtual sites. For lone pair containing heavy atoms, the components of the Drude force constant tensor ($\mathbf{K}_D$) are varied to model the local asymmetry in the electronic response (see eq 2).

Like the virtual site geometry the relative magnitude of the components of $\mathbf{K}_D$ is not part of the parameter fitting function, eq 4. The polarization ESP computed on the aforementioned QM arcs is used to parametrize the components of the force constant tensor. The value of the Drude oscillator charge, initially fit against eq 4 for the LP+ISO model, is scaled as the components of the force constant tensor are varied (keeping the trace approximately constant) until satisfactory agreement with the response curves from QM is found. This yields the LP+ANISO model. The polarization ESP for the resulting model is plotted as the blue-cross curve. By strengthening the polarizability along the LP direction, excellent agreement with the QM response is achieved for the models of acetone, methanol, and methylamine. The response curve for pyridine, which is approximately isotropic, already shows good agreement with the ISO models.

4.2. Interaction Energies. Interaction energies with a single water molecule are computed to probe the hydrogen bonding environment of the model compounds and serve to test the new MM model. In addition, we investigate interactions between the model compounds and a monovalent cation (sodium) to test the model under strong electric field conditions. Comparison to QM interaction energies are made for dimer conformations that correspond to an optimization

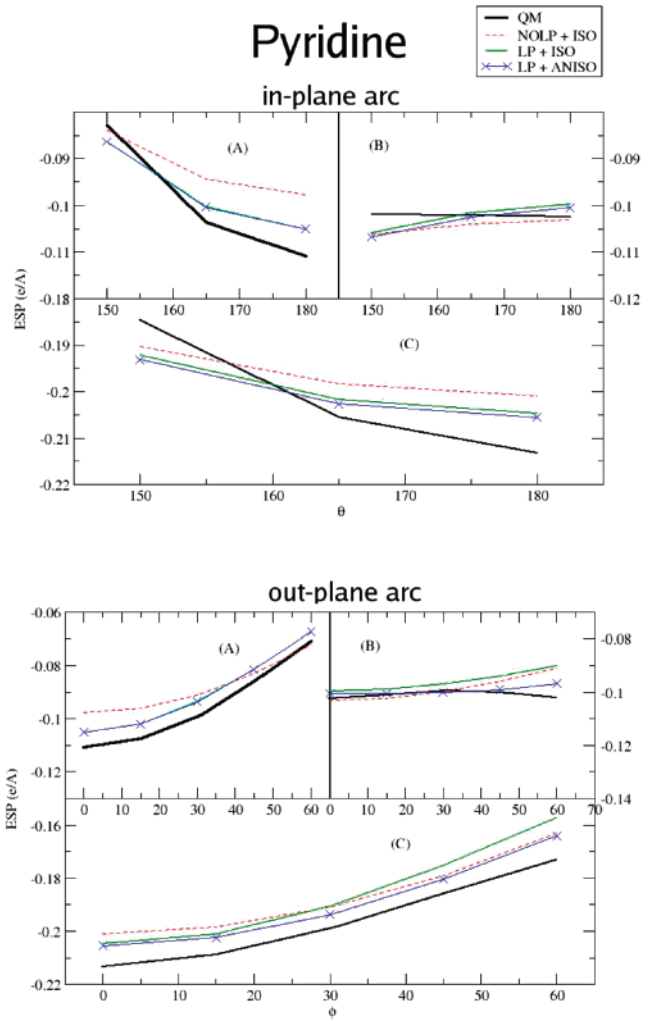

Figure 5. The ESP along an arc 2 Å from the nitrogen of an pyridine monomer is plotted in panel (A). The polarization contribution and total ESP from pyridine in the presence of a 0.5*e* test charge is plotted in panels (B) and (C), respectively. The perturbed ESP is calculated at the position of the 0.5*e* test charge.

along an intermolecular distance coordinate between the oxygen or nitrogen atom of the model compound and the hydrogen bond forming hydrogen of water or sodium ion. The conformations resulting from this partial minimization are presented in Figure 6. The conformation labels indicate whether the water/ion is coincident with the previously defined in-plane or out-plane and the angle θ. The model/sodium conformations (not illustrated) probe the same coordinates.

For water, the results for the optimized energies and the difference between QM and MM are presented in Table 1. The average error over the suite of conformations is presented in Table 2. The results for acetone and methanol illustrate the failure of the NOLP+ISO MM model to predict the location of the lowest energy orientation (coordinated with the lone pair in QM). The LP models (both ISO and ANISO) lead to the correct prediction for the ordering of interaction energies and significantly improve the average error over all conformations. For methylamine a significant improvement is seen in the interaction energies with water. The

Table 1. Interaction Energy and the Energy Difference between QM and MM from a Partial Radial Optimization of a Model Compound/Water Dimer[a]

	QM	NOLP + ISO		LP + ISO		LP + ANISO	
orientation	E_{min}	E_{min}	E_{diff}	E_{min}	E_{diff}	E_{min}	E_{diff}
			Acetone				
in-120	−5.1	−3.8	1.3	−4.7	0.4	−4.9	0.2
in-180	−4.1	−4.0	0.1	−3.6	0.5	−3.6	0.5
out-180	−3.8	−4.0	0.2	−3.7	0.1	−3.7	0.1
			Methanol				
out-105	−4.6	−4.6	0.0	−4.6	0.0	−4.7	0.1
in-105	−4.3	−4.7	0.4	−4.1	0.2	−4.1	0.2
in-180	−2.1	−2.5	0.4	−2.0	0.1	−2.0	0.1
			Methylamine				
in-105	−6.4	−6.5	0.1	−6.2	0.2	−6.4	0.0
out-105	−4.8	−5.4	0.6	−4.5	0.3	−4.6	0.2
in-150	−2.1	−3.5	1.4	−2.3	0.2	−2.3	0.2
			Pyridine				
in-180	−6.3	−6.3	0.0	−6.3	0.0	−6.3	0.0
in-150	−4.9	−5.2	0.3	−5.0	0.1	−5.0	0.1
out-180	−4.4	−5.3	0.9	−4.1	0.3	−4.2	0.1

[a] All energies are in kcal/mol. The orientations correspond to conformations illustrated in Figure 6.

Table 2. Average Error (AE) of MM with Respect to QM for Interaction Energies (kcal/mol) of Model Compound/Water Dimers from Partial Radial Optimization

molecule	NOLP + ISO AE (E_{min})	LP + ISO AE (E_{min})	LP + ANISO AE (E_{min})
acetone	0.6	0.3	0.3
methanol	0.3	0.1	0.1
methylamine	0.7	0.2	0.1
pyridine	0.4	0.1	0.1

energy difference between QM and MM is reduced by greater than 1 kcal/mol for the conformation labeled "in-150", and the average error falls from 0.7 kcal/mol in the NOLP model to 0.2−0.1 kcal/mol for the LP models. A similar improvement is seen with pyridine where the energy difference for the out-of-plane conformation "out-180" is reduced by 0.6−0.8 kcal/mol for the LP models. The addition of anisotropic Drude oscillators gives a modest additional improvement to the observed results leading to smaller energy differences with the QM results relative to the LP+ISO model.

For sodium, the results for the optimized energies and the difference between QM and MM are presented in Table 3. To achieve a satisfactory level of accuracy, it was necessary to place additional LJ interactions centered on the positions of the virtual lone pair sites. The need for such an empirical correction possibly reflects the breakdown of linear response caused by the large distortion in the electron density in the presence of a large electrostatic perturbation. The average errors presented in Table 4 show a marked improvement for the models that use virtual sites relative to the NOLP model. Including anisotropy leads to a further reduction in the average error.

4.3. Linear Response Regime. For polarizable MM models the response of the polarizable degrees of freedom

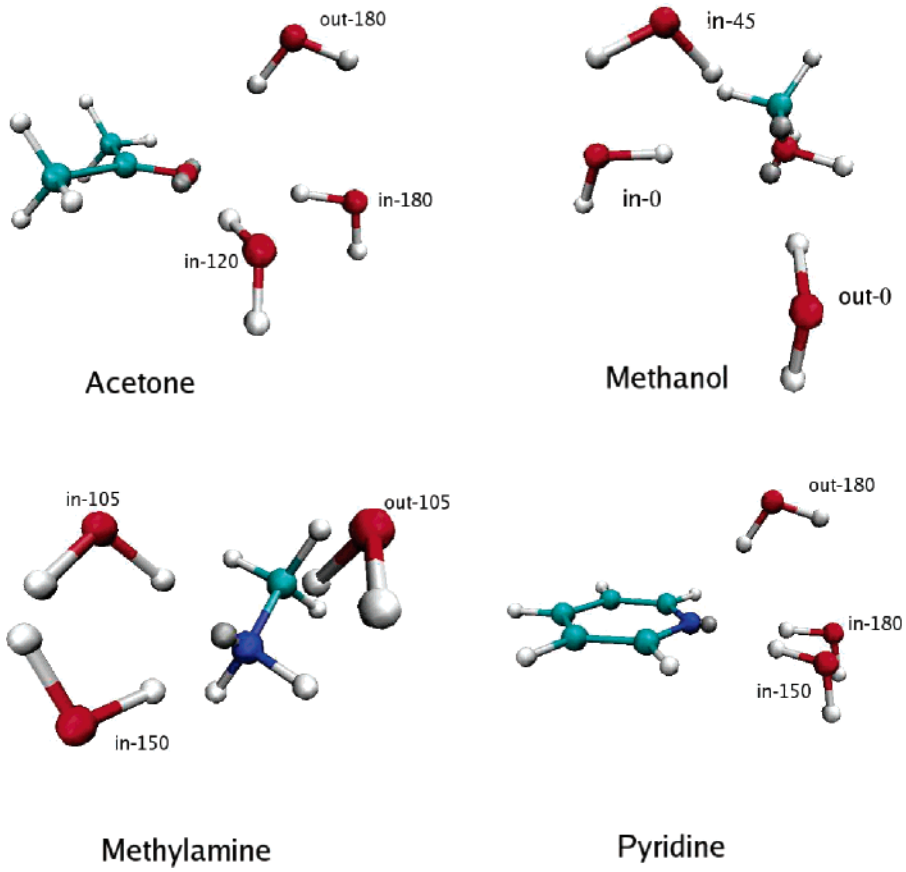

Figure 6. Location of water after partial radial optimization of model compound/water dimer.

Table 3. Interaction Energy and the Energy Difference between QM and MM from a Partial Radial Optimization of a Model Compound/Sodium Dimer[a]

orientation	QM E_{min}	NOLP + ISO E_{min}	NOLP + ISO E_{diff}	LP + ISO E_{min}	LP + ISO E_{diff}	LP + ANISO E_{min}	LP + ANISO E_{diff}
			Acetone				
in-120	−24.5	−24.7	0.2	−24.6	0.1	−24.5	0.0
in-180	−29.9	−31.9	2.0	−30.9	1.0	−29.7	0.2
out-180	−23.2	−25.1	1.9	−23.9	0.7	−24.7	1.5
			Methanol				
in-45	−20.2	−19.6	0.6	−19.8	0.4	−20.9	0.7
in-0	−21.7	−22.1	0.4	−21.2	0.5	−21.5	0.2
out-0	−13.6	−14.2	0.6	−13.5	0.1	−13.7	0.1
			Methylamine				
in-105	−26.2	−26.0	0.2	−26.5	0.3	−27.2	1.0
out-105	−11.9	−15.0	3.1	−13.4	1.5	−13.1	1.2
in-150	−20.8	−21.8	1.0	−22.1	1.3	−21.0	0.2
			Pyridine				
in-180	−29.8	−29.9	0.1	−29.9	0.1	−30.0	0.2
in-150	−25.7	−26.5	0.8	−27.2	1.5	−27.3	1.6
out-180	−23.8	−21.1	2.7	−22.8	1.0	−23.5	0.3

[a] All energies are in kcal/mol. The orientations correspond to conformations similar to those illustrated in Figure 6 for water.

Table 4. Average Error (AE) of MM with Respect to QM for Interaction Energies (kcal/mol) of Model Compound/Sodium Dimers from Partial Radial Optimization

molecule	NOLP + ISO AE (E_{min})	LP + ISO AE (E_{min})	LP + ANISO AE (E_{min})
acetone	1.4	0.6	0.6
methanol	0.5	0.3	0.3
methylamine	1.4	1.0	0.8
pyridine	1.2	0.9	0.7

is typically assumed to be linearly proportional to an electrostatic perturbation. This approximation is exact for a model potential energy that is quadratic in the polarizable degrees of freedom such as polarizable point dipole models[22] and fluctuating charge models[47] where the polarizable degrees of freedom are the magnitude of the dipoles and atomic centered charges, respectively. This condition is not strictly held in the Drude oscillator model, where the electric field is evaluated at the position of the mobile auxiliary particle. For weak perturbations and/or a very stiff spring constant the Drude displacements are much smaller than the interatomic distance (r_{ij}), and the effective response is linear. For large electrostatic perturbations the Drude model, like the real QM molecule, will deviate from linear response. In this nonlinear regime we do not expect the Drude model to successfully model the QM data. Such limitations notwithstanding, the present implementation of the Drude model with a negative (rather than the positive) Drude particle[21,48] does deviate from the linear response regime in the same direction as the real QM case. In this section we investigate the level of accuracy possible with these MM models (both LP models are investigated) by measuring the degree to which the QM molecule response deviates from the linear regime for electrostatic charge perturbations of varying magnitude (0.5*e*, 1.0*e*, 2.0*e*) and compare with the Drude models.

Table 5. Breakdown of Interaction Energy between Acetone and a 0.5*e* Test Charge[a]

model	$q\phi_{stat}$	$0.5q\phi_{pol}$	E^{lr}	E	E_{diff}
		$\theta = 120$, $d = 2.286$ Å			
QM	−10.7	−3.8	−14.5	−14.4	0.1
LP+ISO	−11.2	−2.7	−13.9	−13.9	0.0
LP+ANISO	−11.2	−3.4	−14.6	−14.5	0.1
		$\theta = 180$, $d = 2.1883$ Å			
QM	−13.1	−3.4	−16.5	−16.3	0.2
LP+ISO	−13.4	−3.4	−16.8	−16.7	0.1
LP+ANISO	−13.4	−3.3	−16.7	−16.6	0.1

[a] All values are in kcal/mol. Calculations for conformations at $\theta =$ 120 and $\theta = 180$ are presented. Shown are the static ($q\phi_{stat}$) and polarization ($0.5q\phi_{pol}$) contribution to the energy predicted from linear response (E^{lr}), the actual interaction energy (E), and the difference between them (E_{diff}). The models presented include the QM molecule and the LP+ISO and LP+ANISO Drude oscillator models.

The total interaction energy between a polarizable molecule and a test charge (q_{test}) can be written as

$$E = \int_0^{q_{test}} dq\, \phi(q) \tag{6}$$

where $\phi(q)$ is the total electrostatic potential from the molecule at the position of the perturbing charge. In the linear response approximation, it is assumed that $\phi(q) = A + Bq$, and the interaction energy becomes

$$E^{lr} = Aq_{test} + \frac{1}{2}Bq_{test}^{\ 2} \tag{7}$$

The constant A corresponds to the electrostatic potential in the absence of a perturbing charge, $\phi_{stat} = \phi(q = 0)$. The constant B, a measure of the change in the electrostatic potential to the presence of a test charge, is thus $(\phi(q_{test}) - \phi_{stat})/q_{test}$ which is equal to ϕ_{pol}/q_{test}. The computation of E^{lr} follows from a similar breakdown of the ESP into static (ϕ_{stat}) and polarization (ϕ_{pol}) contributions performed in the electrostatic model parametrization (see section 2.2). A series of single point calculations of the ESP are carried out at positions corresponding to the minimum energy for the model compound/sodium dimer. The static field contribution to E^{lr}, corresponding to the first term in eq 7, is taken from the ESP in the absence of a test charge. The contribution to E^{lr} from polarization, the second term in eq 7, is taken from the difference in the ESP in the presence and absence of a test charge. To examine the validity of linear response, the computed value for E^{lr} is compared to the actual QM interaction energy, taken as the difference between the energy of the complex and the energy of the monomer. The results were particularly sensitive to the basis set chosen. Therefore the results for a large basis set including diffuse and polarization functions (6-311+G(3df,2p)) is presented in this article. Along with the interaction energy (E and E^{lr}) the aforementioned static and polarization components of E^{lr} are recorded for acetone in Tables 5−7 for the 0.5*e*, 1.0*e*, and 2.0*e* charge, respectively. The conformations corresponding to the in-120 and in-180 labels are similar to those plotted for the model compound/water dimer (see Figure 6). The same calculations were then carried out for the LP+ISO and LP+ANISO MM models.

Table 6. Breakdown of Interaction Energy between Acetone and a 1.0*e* Test Charge[a]

model	$q\phi_{stat}$	$0.5q\phi_{pol}$	E^{lr}	E	E_{diff}
		$\theta = 120$, $d = 2.286$ Å			
QM	−21.3	−19.3	−40.6	−38.0	2.6
LP+ISO	−22.3	−11.8	−34.1	−33.6	0.5
LP+ANISO	−22.5	−15.8	−38.3	−36.9	1.4
		$\theta = 180$, $d = 2.1883$ Å			
QM	−26.2	−15.3	−41.5	−40.2	1.3
LP+ISO	−26.8	−14.9	−41.7	−40.7	1.0
LP+ANISO	−26.8	−14.2	−41.0	−40.2	0.8

[a] All values are in kcal/mol. Calculations for conformations at $\theta =$ 120 and $\theta = 180$ are presented. Shown are the static ($q\phi_{stat}$) and polarization ($0.5q\phi_{pol}$) contribution to the energy predicted from linear response (E^{lr}), the actual interaction energy (E), and the difference between them (E_{diff}). The models presented include the QM molecule and the LP+ISO and LP+ANISO Drude oscillator models.

Table 7. Breakdown of Interaction Energy between Acetone and a 2.0*e* Test Charge [a]

model	$q\phi_{stat}$	$0.5q\phi_{pol}$	E^{lr}	E	E_{diff}
		$\theta = 120$, $d = 2.286$ Å			
QM	−42.9	−151.0	−193.9	−146.7	47.2
LP+ISO	−44.7	−56.3	−101.0	−94.6	6.4
LP+ANISO	−44.7	−130.1	−174.8	−124.9	49.9
		$\theta = 180$, $d = 2.1883$ Å			
QM	−52.4	−115.0	−167.4	−128.8	38.6
LP+ISO	−53.7	−78.4	−132.1	−119.1	13.0
LP+ANISO	−53.6	−71.1	−124.7	−115.0	9.7

[a] All values are in kcal/mol. Calculations for conformations at $\theta =$ 120 and $\theta = 180$ are presented. Shown are the static ($q\phi_{stat}$) and polarization ($0.5q\phi_{pol}$) contribution to the energy predicted from linear response (E^{lr}), the actual interaction energy (E), and the difference between them (E_{diff}). The models presented include the QM molecule and the LP+ISO and LP+ANISO Drude oscillator models.

For the 0.5*e* charge, linear response holds almost exactly in both the QM and MM calculations. As expected, from fitting to the ESP, the LP+ANISO model improves the accuracy of the polarization contribution to the interaction energy and gives the best overall agreement with the QM result. For the 1.0*e* test charge, the energies begin to deviate by approximately 0.5−2.5 kcal/mol from the linear response regime. Somewhat encouraging is that the deviation in the interaction energy caused by nonlinear effects arising from finite Drude displacements in the MM model are in the same direction as the QM calculation. Only the LP+ANISO model gives interaction energies that lie within the linear response resolution.

For the 2.0*e* charge, the deviations from linear response become quite severe (≈50 kcal/mol). The large deviations would appear to reflect poorly on the effectiveness of linear response models (point dipole and fluctuating charge) and approximate linear response model (Drude oscillators) to accurately model interactions with divalent ions such as calcium and magnesium. However one should keep in mind that this experiment is performed in the gas phase. As noted in previous work,[20,35,49] contributions to the electronic response in the gas phase from diffuse portions of the electron wave function are reduced in a condensed phase

environment due to repulsive interactions with neighboring molecules. It may be the case that this would decrease not only the polarizability but also the degree to which the response of these molecules deviates from the linear response regime. If these deviations are indicative of the response in aqueous ionic systems, it may be necessary to incorporate additional features (e.g. an anharmonic restoring force to the Drude particles) to properly model the polarization effects when linear response breaks down.

4.4. Conclusions. In the present manuscript we investigate the components of the electrostatic potential, in the vicinity of functional groups containing lone pairs, for a set of small molecules. Included are the nitrogen of pyridine and methylamine, the carbonyl group of acetone, and the hydroxyl group of methanol. Three models, incorporating virtual sites to represent the lone pairs and the local polarization anisotropy, were parametrized and compared with ab initio electronic structure calculations for a system containing the molecule and a perturbing charge of magnitude $+0.5e$. Use of virtual sites representing lone pairs and anisotropic atom-based polarizabilities allows for the model to better reproduce the anisotropy of interactions with the environment, thereby improving the ability of the model to reproduce atomic detail interactions. Only the model using both virtual sites and anisotropic Drude oscillators is able to capture all the features of the local QM electrostatic potential. Dimer energies with water and sodium show a marked improvement for models that incorporate virtual sites in the representation of lone pairs relative to QM calculations. The MM model that incorporates virtual sites and anisotropic atomic polarizabilities for lone pairs will be implemented into an empirical force field that explicitly includes electronic polarizability via Drude oscillators.

Notably absent from the preceding analysis is a water model. Although water does indeed have lone pairs, the use of a TIP4P-like[50] virtual site (charge on oxygen is shifted off the atom along the HOH bisector) by the Drude water model (SWM4-NDP[20]) that will accompany the rest of the biomolecular force field appears to provide the level of detail necessary to accurately reproduce the water dimer geometry. Furthermore the nearly isotropic experimental molecular polarizability[51] of water appears to make the addition of an anisotropic Drude oscillator unnecessary for this molecule.

Acknowledgment. Financial support to A.D.M. is acknowledged from the NIH (GM 51501) and to B.R. and A.D.M. from the NIH (GM 072558). Computer time allocations were received from DOD ACS Major Shared Resource Computing and PSC Pittsburgh Supercomputing Center. E.H. would like to thank Troy Whitfield and Sergey Krupin for helpful discussions.

Supporting Information Available: The model parameters, minimized interacting dimer distances, and energies. This material is available free of charge via the Internet at http://pubs.acs.org.

References

(1) MacKerell, A. D., Jr.; Bashford, D.; Bellott, M.; Dunbrack, R. L., Jr.; Evanseck, J. D.; Field, M. J.; Fisher, S.; Gao, J.; Guo, H.; Ha, S.; Joseph-McCarthy, D.; Kuchnir, L.; Kuczera, K.; Lau, F. T. K.; Mattos, C.; Michnick, S.; Ngo, T.; Nguyen, D. T.; Prodhorn, B.; Reiher, W. E., III; Roux, B.; Schlenkrich, M.; Smith, J. C.; Stote, R.; Straub, J.; Watanabe, M.; Wirkiewicz-Kuczera, D.; Yin, D.; Karplus, M. *J. Phys. Chem. B* **1998**, *102*, 3586−3616.

(2) Jorgensen, W. L.; Maxwell, D. S.; Tirado-Rives, J. *J. Am. Chem. Soc.* **1996**, *118*, 11225−11236.

(3) Cornell, W. D.; Cieplak, P.; Bayly, C. I.; Gould, I. R.; Jr., K. M. M.; Ferguson, D. M.; Spellmeyer, D. C.; Fox, T.; Caldwell, J. W.; Kollman, P. A. *J. Am. Chem. Soc.* **1995**, *117*, 5179−5197.

(4) van Gunsteren, W. F.; Billeter, S. R.; Eising, A. A.; Huenenberger, P. H.; Krueger, P.; Mark, A. E.; Scott, W. R. P.; Tironi, I. G. *Biomolecular Simulation: The GROMOS96 Manual and User Guide*; Hochshulverlag AG/ETH: Zurich, 1996.

(5) Silvestrelli, P. L.; Parrinello, M. *J. Chem. Phys.* **1999**, *111*, 3572−3580.

(6) Harder, E.; Eaves, J. D.; Tokmakoff, A.; Berne, B. J. *Proc. Natl. Acad. Sci.* **2005**, *102*, 11611−11616.

(7) Asbury, J. B.; Steinel, T.; Kwak, K.; Corcelli, S. A.; Lawrence, C. P.; Skinner, J. L.; Fayer, M. D. *J. Chem. Phys.* **2004**, *121*, 12431−12446.

(8) Xu, H.; Stern, H. A.; Berne, B. J. *J. Phys. Chem. B* **2002**, *106*, 2054−2060.

(9) Stuart, S. J.; Berne, B. J. *J. Phys. Chem.* **1996**, *100*, 11934−11943.

(10) Jungwirth, P.; Tobias, D. J. *J. Phys. Chem. B* **2002**, *106*, 6361−6373.

(11) Herce, D. H.; Perera, L.; Darden, T. A.; Sagui, C. *J. Chem. Phys.* **2005**, *122*, 024513.

(12) Archontis, G.; Leontidis, E.; Andreou, G. *J. Phys. Chem. B* **2005**, *109*, 17957−17966.

(13) Lamoureux, G.; Roux, B. *J. Phys. Chem. B* **2006**, *110*, 3308−3322.

(14) Noskov, S. Y.; Lamoureux, G.; Roux, B. *J. Phys. Chem. B* **2005**, *109*, 6705−6713.

(15) Vorobyov, I. V.; Anisimov, V. M.; MacKerell, A. D., Jr. *J. Phys. Chem. B* **2005**, *109*, 18988−18999.

(16) Kim, B.; Young, T.; Harder, E.; Friesner, R. A.; Berne, B. J. *J. Phys. Chem. B* **2005**, *109*, 16529−16538.

(17) Allen, T. W.; Andersen, O. S.; Roux, B. *Biophys. J.* **2006**, *90*, 3447−3468.

(18) Allen, T. W.; Andersen, O. S.; Roux, B. *Proc. Natl. Acad. Sci.* **2004**, *101*, 117−122.

(19) Lamoureux, G.; Roux, B. *J. Chem. Phys.* **2003**, *119*, 3025−3039.

(20) Lamoureux, G.; MacKerell, A. D., Jr.; Roux, B. *J. Chem. Phys.* **2003**, *119*, 5185−5197.

(21) Anisimov, V. M.; Lamoureux, G.; Vorobyov, I.; Huang, N.; Roux, B.; MacKerell, A. D., Jr. *J. Chem. Theory Comput.* **2005**, *1*, 153−168.

(22) van Belle, D.; Froeyen, M.; Lippens, G.; Wodak, S. J. *Mol. Phys.* **1992**, *77*, 239−255.

(23) Bernardo, D. N.; Ding, Y.; Krogh-Jespersen, K.; Levy, R. M. *J. Phys. Chem.* **1994**, *98*, 4180−4187.

(24) Mountain, R. D. *J. Chem. Phys.* **1995**, *103*, 3084−3090.

(25) Gao, J.; Habibollazadeh, D.; Shao, L. *J. Phys. Chem.* **1995**, *99*, 16460−16467.

(26) Dang, L. X.; Chang, T. *J. Chem. Phys.* **1997**, *106*, 8149−8159.

(27) Kaminski, G. A.; Stern, H. A.; Berne, B. J.; Friesner, R. A.; Cao, Y. X.; Murphy, R. B.; Zhou, R.; Halgren, T. A. *J. Comput. Chem.* **2002**, *23*, 1515−1531.

(28) Drude, P. *The Theory of Optics*; Longmans: Green, New York, 1902.

(29) Thole, B. T. *Chem. Phys.* **1981**, *59*, 341−350.

(30) van Duijnen, P. T.; Swart, M. *J. Phys. Chem. A* **1998**, *102*, 2399−2407.

(31) MacKerell, A. D., Jr.; Brooks, B.; Brooks, C. B., III; Nilsson, L.; Roux, B.; Won, Y.; Karplus, M. *CHARMM: The Energy Function and Its Parametrization with an Overview of the Program. In Encyclopedia of Computational Chemistry*; John Wiley & Sons: Chichester, 1998; Vol. 1.

(32) Banks, J. L.; Kaminski, G. A.; Zhou, R.; Mainz, D. T.; Berne, B. J.; Friesner, R. A. *J. Chem. Phys.* **1999**, *110*, 741−754.

(33) Stern, H. A.; Kaminski, G. A.; Banks, J. L.; Zhou, R.; Berne, B. J.; Friesner, R. A. *J. Phys. Chem. B* **1999**, *103*, 4730−4737.

(34) Liu, Y.-P.; Kim, K.; Berne, B. J.; Friesner, R. A.; Rick, S. W. *J. Chem. Phys.* **1998**, *108*, 4739−4755.

(35) Stern, H. A.; Berne, B. J.; Friesner, R. A. *J. Chem. Phys.* **2001**, *115*, 2237−2251.

(36) Singh, U. C.; Kollman, P. A. *J. Comput. Chem* **1984**, *5*, 129−145.

(37) Singh, U. C.; Kollman, P. A. *J. Phys. Chem.* **1993**, *97*, 10269−10280.

(38) Yin, D. Ph.D. Thesis, University of Maryland, 1997.

(39) Chen, I.-J.; Yin, D.; MacKerell, A. D., Jr. *J. Comput. Chem* **2002**, *23*, 199−213.

(40) Miller, K. J. *J. Am. Chem. Soc.* **1990**, *112*, 8533−8542.

(41) Bader, R. F. W. *Atoms in Molecules − A Quantum Theory*; Oxford University Press Inc.: New York, 1990.

(42) Frisch, M. J.; Trucks, G. W.; Schlegel, H. B.; Scuseria, G. E.; Robb, M. A.; Cheeseman, J. R.; Montgomery, J. A., Jr.; Vreven, T.; Kudin, K. N.; Burant, J. C.; Millam, J. M.; Iyengar, S. S.; Tomasi, J.; Barone, V.; Mennucci, B.; Cossi, M.; Scalmani, G.; Rega, N.; Petersson, G. A.; Nakatsuji, H.; Hada, M.; Ehara, M.; Toyota, K.; Fukuda, R.; Hasegawa, J.; Ishida, M.; Nakajima, T.; Honda, Y.; Kitao, O.; Nakai, H.; Klene, M.; Li, X.; Knox, J. E.; Hratchian, H. P.; Cross, J. B.; Bakken, V.; Adamo, C.; Jaramillo, J.; Gomperts, R.; Stratmann, R. E.; Yazyev, O.; Austin, A. J.; Cammi, R.; Pomelli, C.; Ochterski, J. W.; Ayala, P. Y.; Morokuma, K.; Voth, G. A.; Salvador, P.; Dannenberg, J. J.; Zakrzewski, V. G.; Dapprich, S.; Daniels, A. D.; Strain, M. C.; Farkas, O.; Malick, D. K.; Rabuck, A. D.; Raghavachari, K.; Foresman, J. B.; Ortiz, J. V.; Cui, Q.; Baboul, A. G.; Clifford, S.; Cioslowski, J.; Stefanov, B. B.; Liu, G.; Liashenko, A.; Piskorz, P.; Komaromi, I.; Martin, R. L.; Fox, D. J.; Keith, T.; Al-Laham, M. A.; Peng, C. Y.; Nanayakkara, A.; Challacombe, M.; Gill, P. M. W.; Johnson, B.; Chen, W.; Wong, M. W.; Gonzalez, C.; Pople, J. A. *Gaussian 03, Revision C.02*; Gaussian Inc.: Pittsburgh, PA.

(43) Huang, N.; MacKerell, A. D., Jr. *J. Phys. Chem. B* **2002**, *106*, 7820−7827.

(44) Becke, A. D. *Phys. Rev. A* **1988**, *38*, 3098−3100.

(45) Lee, C.; Yang, W.; Parr, R. G. *Phys. Rev. B* **1988**, *37*, 785−789.

(46) Boys, S.-F.; Bernardi, F. *Mol. Phys.* **2002**, *100*, 65−73.

(47) Rick, S. W.; Stuart, S. J.; Berne, B. J. *J. Chem. Phys.* **1994**, *101*, 6141−6156.

(48) Lamoureux, G.; Harder, E.; Vorobyov, I. V.; Roux, B.; MacKerell, A. D., Jr. *Chem. Phys. Lett.* **2006**, *418*, 245−249.

(49) Morita, A.; Kato, S. *J. Chem. Phys.* **1999**, *110*, 11987−11998.

(50) Jorgensen, W. L.; Chandrasekhar, J.; Madura, J. D.; Impey, R. W.; Klein, M. L. *J. Chem. Phys.* **1983**, *79*, 926−935.

(51) Murphy, W. F. *J. Chem. Phys.* **1977**, *67*, 5877−5882.

CT600180X